tvst

Cornea & External Disease

Portable Anterior Eye Segment Imaging System for Teleophthalmology

Ana Diego[1] **and Mohamed Abou Shousha**[1,2]

[1] Department of Biomedical Engineering, University of Miami, Miami, FL, USA
[2] Bascom Palmer Eye Institute, University of Miami Health System, Miami, FL, USA

Correspondence: Mohamed Abou Shousha, Bascom Palmer Eye Institute, University of Miami, 900 Northwest 17th Street, Floor 3, Miami, FL 33136, USA. e-mail: mshousha@med.miami.edu

Received: May 24, 2022
Accepted: November 8, 2022
Published: January 6, 2023

Keywords: telemedicine; teleophthalmology; wearable headsets; anterior eye segment

Citation: Diego A, Abou Shousha M. Portable anterior eye segment imaging system for teleophthalmology. Transl Vis Sci Technol. 2023;12(1):11, https://doi.org/10.1167/tvst.12.1.11

Objective: This study aims to compare a new prototype for a portable anterior eye segment imaging system with the standard method for ophthalmology examination.

Methods: The new imaging system consisted of two IMX219 Arducam autofocus sensors (Arducam, China, Nanjing) for Raspberry Pi V2 camera module connected to a Raspberry Pi Zero W (Raspberry Pi Foundation, UK, Cambridge) that clips to a wearable headset. The 2D videos of the anterior eye segment were recorded with the new system and a 720p FaceTime HD camera (Apple, Cupertino, CA). Afterward, ophthalmologists evaluated the videos using a standard clinical eye examination form. These evaluations were compared with the standard slit-lamp clinical assessment performed during the patient's visit.

Results: Thirty-five eyes were evaluated. The sensitivity and specificity percentages were statistically significant between the two imaging modalities ($P \leq 0.001$). The evaluations performed from videos obtained with the new imaging system had better sensitivity and specificity percentages overall. However, statistically significant differences were only observed in cornea, anterior chamber, iris, and lens.

Conclusions: Specificity percentages were higher than sensitivity percentages in both imaging modalities, indicating that video evaluations are less accurate for pathological screening. Nevertheless, the new system evaluations were significantly better than the webcam evaluations.

Translational Relevance: This study presented an alternative system to assess eye conditions for telemedicine, one that provides more details than the current standard and uses new wearable headsets technologies.

Introduction

Telemedicine presents an alternative to traditional face-to-face medical consultations. Teleophthalmology increases access to ophthalmic care in rural areas where specialists are few. In addition, teleophthalmology lowers screening barriers and facilitates diagnosis follow-ups.[1] Moreover, during the coronavirus disease 2019 (COVID-19) pandemic, telemedicine systems were required to continue providing healthcare standards. Leading telehealth platforms reported an increase in virtual patient visits from 257% to almost 700% because of the pandemic.[2] However, the most used method for teleophthalmology constituted video visits and eye evaluations through computer web cameras. Even though web cameras are a widely available technology, the quality of the images, the room lighting, and camera focus limits doctors' ability to evaluate eye conditions. Therefore, there is a need to develop accurate and reliable teleophthalmic systems and methods that achieve the accuracy of in-person examinations.[3]

Anterior and posterior eye segment imaging constitutes a fundamental tool for ophthalmic diagnosis and a necessary component in teleophthalmology. However, clinical imaging devices are complex, not portable, and require trained clinical technicians. The current imaging systems used in teleophthalmology include smartphones, compact mobile cameras with lens adaptors, and computer web cameras.[4–6] Several studies compared the diagnostic capabilities of images

from portable cameras with pictures taken with the clinical gold standard devices. Although there is a wide range of sensitivity and specificity values, these studies show the promising application of portable imaging systems to diagnose anterior eye segment conditions.[7,8]

On the other hand, portable devices available for teleophthalmology also require another person's assistance to maintain them correctly positioned during imaging and testing. Additionally, several mobile devices target a specific test or imaging technique. Therefore, our research group intends to develop a comprehensive ophthalmic diagnostic tool that allows the autonomous testing of a patient's eye conditions. We propose the application of headset technologies as a potential solution. The users can comfortably wear them, and they have strong computer capabilities and specialized optical elements and cameras, making them an excellent option for teleophthalmology applications.

The computer technology of the latest virtual reality/augmented reality (VR/AR) headsets allows the development of several software applications for teleophthalmology, from visual field testing to vision augmentation (Goldbach, et al. IOVS 2021;62: ARVO E-Abstract 1017; Kashem, et al. IOVS 2021;62: ARVO E-Abstract 33189). However, obtaining images of the eye requires external high-quality cameras. This paper discusses the development of a wearable camera system for anterior eye segment imaging. In addition, this study assesses the accuracy and reliability of spot diagnosis of anterior eye segment pathologies by specialized ophthalmologists using 2D videos recorded with the new wearable camera system and 2D videos recorded with regular web camera. These evaluations are compared with the standard slit lamp biomicroscope assessment performed during the clinical visit. The purpose of this study is to validate the application of this new system as an improved teleophthalmology evaluation tool for anterior segment examinations.

Methods

Study Design

The research represents a clinic-based comparative study. The University of Miami Institutional Review Board reviewed the study protocol to verify it followed the ethical guidelines for research involving humans established on the Declaration of Helsinki and the Health Insurance Portability and Accountability Act (HIPAA). Patients were recruited from Bascom Palmer Eye Institute, Miami, Florida, at their scheduled clinical consults. Patients' inclusion criteria were not based on the presence or absence of pathology and eye dilation. The eyes evaluated in the study corresponded to the eye examined by the clinician during the visit. Participants were eligible to be included in the study if they were over 18 years old and were willing and able to sign the informed consent form. Twenty patients agreed to participate in the study, and 35 eyes were assessed by the attending doctor during the clinical visit. A total of 70 videos were recorded using the wearable headset camera system and the computer webcam. The patients were recruited from the clinic of 2 anterior eye segment ophthalmologists, and the 2D videos recorded were later divided and sent to 4 other ophthalmologists for evaluation.

Figure 1. Side view of camera mount attached to HoloLens 2 display.

Imaging System

The wearable headset camera system for anterior eye segment imaging developed for this study consists of two Arducam autofocus sensors (Arducam, China, Nanjing) for Raspberry Pi V2 camera module connected to a Raspberry Pi Zero W (Raspberry Pi Foundation, UK, Cambridge) attached to a HoloLens 2 (Microsoft, Redmond, WA). The camera mount prototype clips on the glasses, as shown in Figures 1 and 2. This prototype can be manually adjusted to acquire a centered view of the eye through a system of hinges, a ball-and-socket articulation, and the HoloLens 2 visor mechanism. The latter allows the glasses' display to be removed from the field of view of the camera when the imaging test is required. The cameras possess a one fourth in 8 MP IMX219 autofocus lens sensor with an effective focal length of 2.8 mm. However, the videos were recorded at 30 frame per seconds with an image resolution of 1080p using the H264 encoder to support Raspberry Pi Zero W

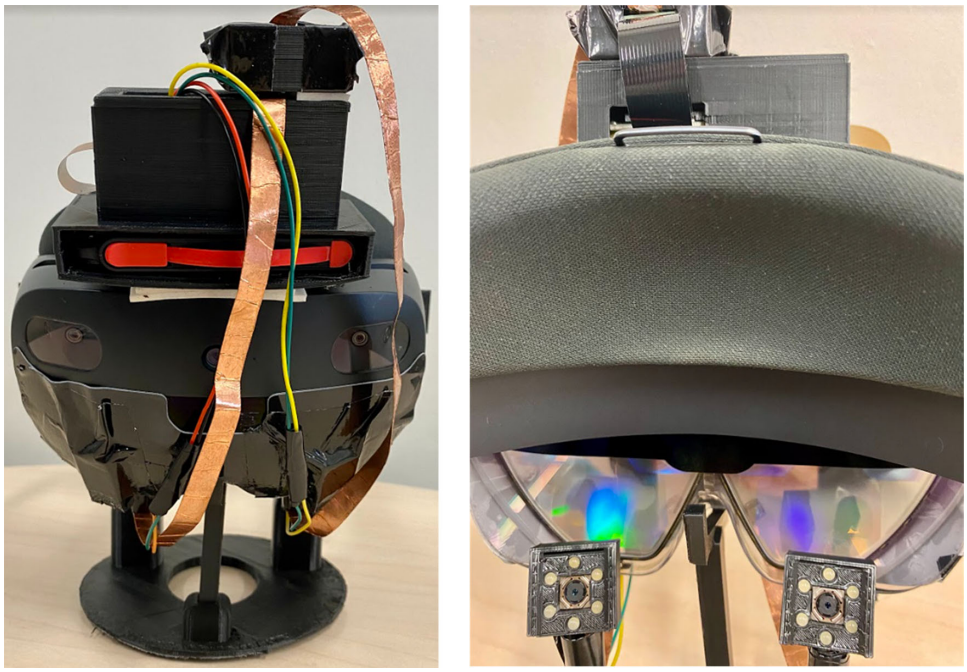

Figure 2. Front view and inside view of the camera mount attached to HoloLens 2 display.

video processing memory. These camera specifications allowed a magnification of × 0.069. A secure VNC connection allowed users to control the Raspberry Pi Zero W from a local computer and preview the camera's feedback to adjust its position and focus. In addition, six diffused white LEDs were added to the camera to improve illumination while imaging the eyes. The code written to control the camera and the LEDs was developed in Python (Python Software Foundation, Wilmington, DE).

On the other hand, to introduce this new imaging system as an alternative option for telemedicine, videos were also recorded with computer webcams, the standard method used during the COVID-19 pandemic to perform the video visits. The computer used to record the videos was a 2012 MacBook Pro with a 720p FaceTime HD camera (Apple, Cupertino, CA). The images acquired had a resolution of 1280 × 720 and a magnification of × 0.0205. Room lighting was used for imaging with the web camera. To standardize illumination conditions the same clinical room was utilized, all the windows were closed, and all the room lights were on when recording started.

Imaging Protocol

First, doctors evaluated the patient during the clinical visit with the traditional slit-lamp biomicroscope. Afterward, a research fellow explained to the patients how to correctly position the wearable headset. Because this study utilized the first prototype for the wearable imaging system, and the autonomous image acquisition and camera positioning modules are still under development, the research fellow had to also assist the patients in acquiring the images and repositioning the system to improve image quality.

The researcher positioned the HoloLens glasses on the patient's head with the display flipped upward to set the cameras at eye level, as seen in Figure 3. The research fellow accessed the Raspberry Pi Zero on an external local computer to record and view the live camera feedback. Based on the camera feedback, the headset and camera position were adjusted to center the eye image in the preview frame. The computer program recorded 2D videos one at a time, starting with the right eye, and turned-on corresponding LEDs while recording. Each video lasted about 1 minute. The camera is programmed to focus automatically, but manual focusing with the keyboard is also available in case the camera position changed or if the best focus was not achieved after the autofocus trial. In addition, the researcher could adjust LEDs' brightness before starting recording based on the patient's mydriasis status or if the patient complained about light sensitivity. The researcher indicated the patient to move the eyes up, down, right, left, and center. Movement of the eyes while recording was standardized for both headset and web camera

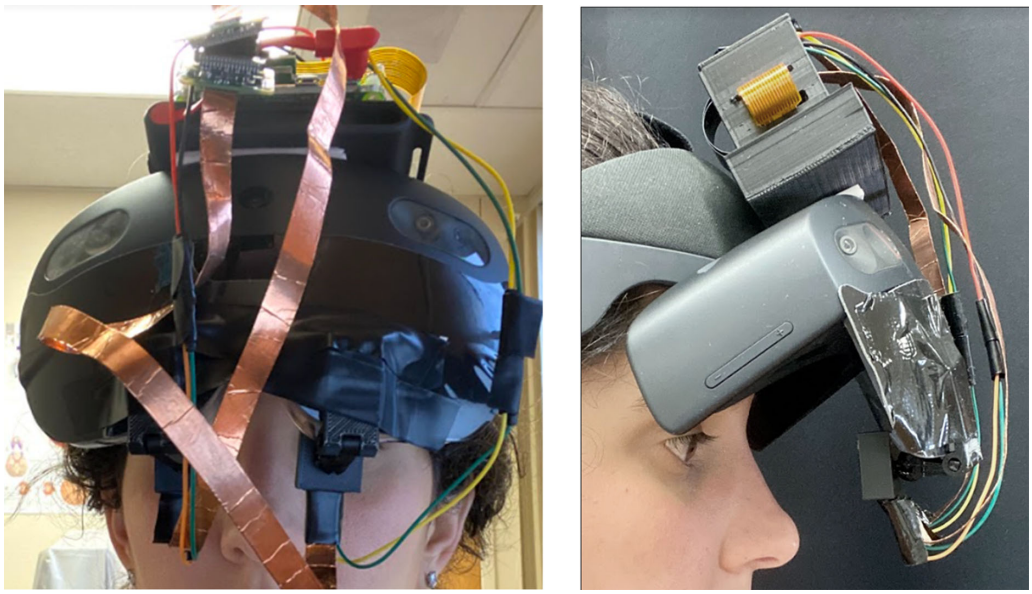

Figure 3. Front view and side view of user wearing headset camera system.

Figure 4. Example of eye image taken with the headset camera system (*left*) and image with the web camera (*right*).

systems. Because the camera position for both imaging modalities is fixed while recording, moving the eyes allowed a better evaluation, and increased recording time.

Next, the fellow asked the patient to come closer to the computer web camera. The position of the web camera had to be adjusted to get a centered image of the eye. Because a laptop built-in web camera was used, the display angle and the height of the laptop with respect to the patient position were modified if required. On the camera preview, a green rectangle was added to serve as a guide to position the patient's eyes, the purpose was to keep the eyes within the rectangle while recording. The patient was directed to look straight into the camera's green light at first for positioning. During recording, the fellow asked the patient to move the eyes up, down, right, left, and center, as previously done with headset system. Another program developed in MATLAB (MathWorks, Natick, MA) recorded 2D web camera videos.

For all the patients, the videos with the wearable headset were recorded first followed by the web camera recordings. This order was determined to save time in case a patient was called for another appointment, because the new imaging prototype required more time to setup. In addition, recording the web camera videos was faster because the patients were more familiar with this technology. Examples of the images acquired with both imaging systems are presented in Figures 4, 5, and 6.

Image Grading

Google Forms platform was used to create a questionnaire to evaluate the videos. The headset and

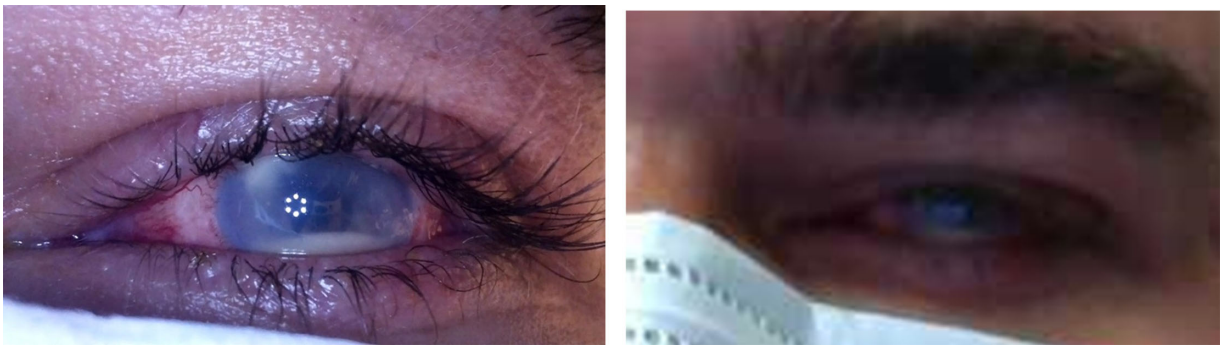

Figure 5. Example of eye image taken with the headset camera system (*left*) and image with the web camera (*right*).

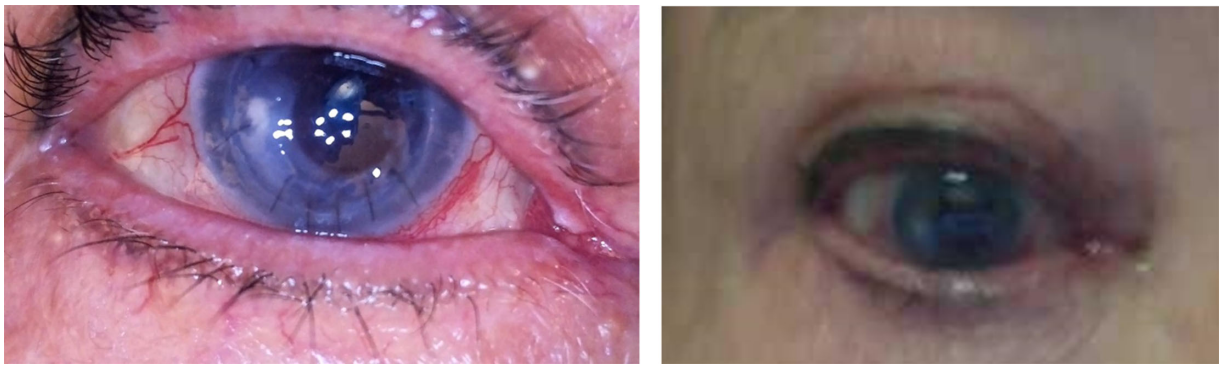

Figure 6. Example of eye image taken with the headset camera system (*left*) and image with the web camera (*right*).

web camera videos were randomly added in the form to minimize bias that can arise from video presentation order. The developed questionnaire followed the format of eye physical examination forms in the electronic clinical records. An example of the form created is presented in Figures 7 and 8. Each section in the form corresponded to an eye video, and each question in the section asked to evaluate one of the following ocular structures: external, lids and lashes, conjunctiva and sclera, cornea, anterior chamber, iris, and lens. Each section alternated between the wearable systems videos and web camera videos of different patients. A set of checkboxes with corresponding pathologies was presented to the grader to select for each feature. These pathologies are included in the electronic chart that the doctors use during an eye physical examination, Figure 9 shows an example of the standard examination form for the cornea. In addition, a final question asked the grader to evaluate video quality following a 5-point graded scale previously validated in a study that compared a smartphone ophthalmic imaging adaptor.[9] This graded scale is based on the doctors' ability to exclude emergent findings from videos or images. The criteria followed (1) inadequate for any diagnostic purpose; (2) unable to exclude all emergent findings; (3) only able to exclude emergent findings; (4) not ideal but still able to exclude subtle findings; and (5) ideal quality. The videos were divided and re-evaluated by four ophthalmologists. These doctors did not examine the patient with the slit lamp during their clinical appointment.

Statistical Analysis

The first step in analyzing the results involved collecting responses from the Google Forms questionnaire previously described. The responses were divided into six categories: true negatives (TNs); true positives (TPs); false negatives (FNs); false positives (FPs); unable to tell (UT); and other conditions (OCs). TN included those responses that correctly identified the absence of a condition compared to the clinical chart evaluations. TP represented the responses that correctly identified the presence of a condition. FN and FP were associated with the evaluations that failed to identify a condition's absence and presence, respectively. The UT category designated to responses where the grader considered that the video did not allow the evaluation

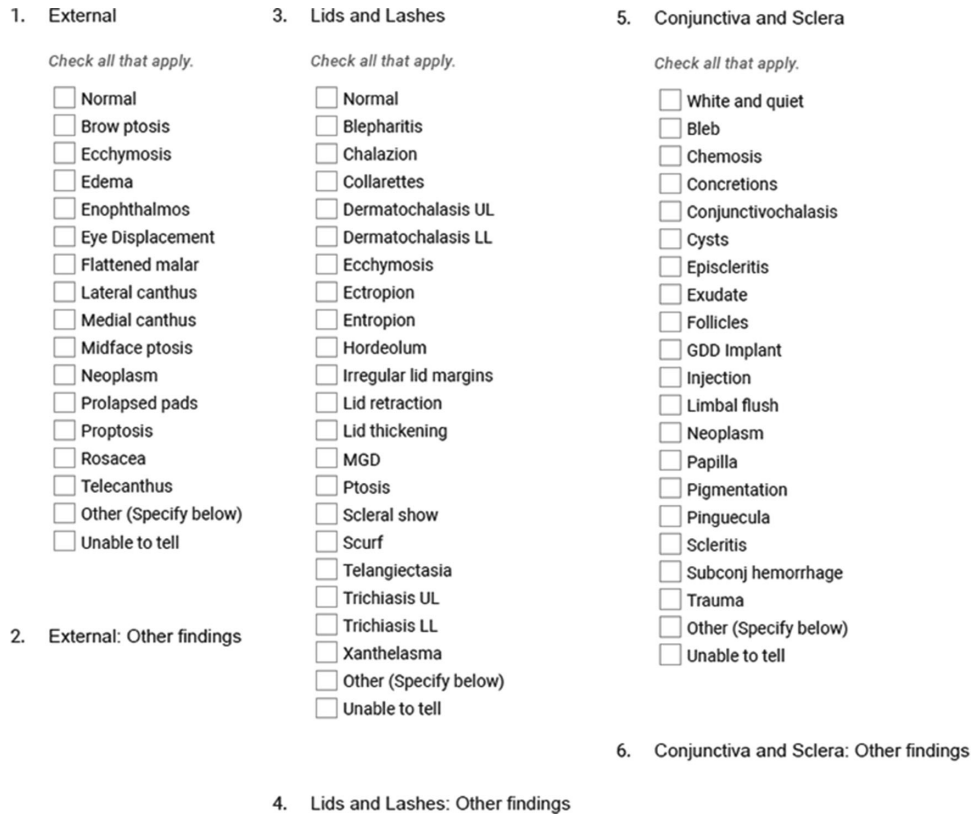

Figure 7. Example of evaluation form for eye structures: external, lids and lashes, and conjunctiva.

of an ocular feature. Last, the OC category included the responses where the grader recognized the presence of a condition but misidentified the type of condition concerning the evaluation in the clinical chart. The sensitivity and specificity of the evaluations were calculated to assess the imaging modalities' validity for assessing anterior eye segment features. In addition, the percentage sensitivity and specificity per feature

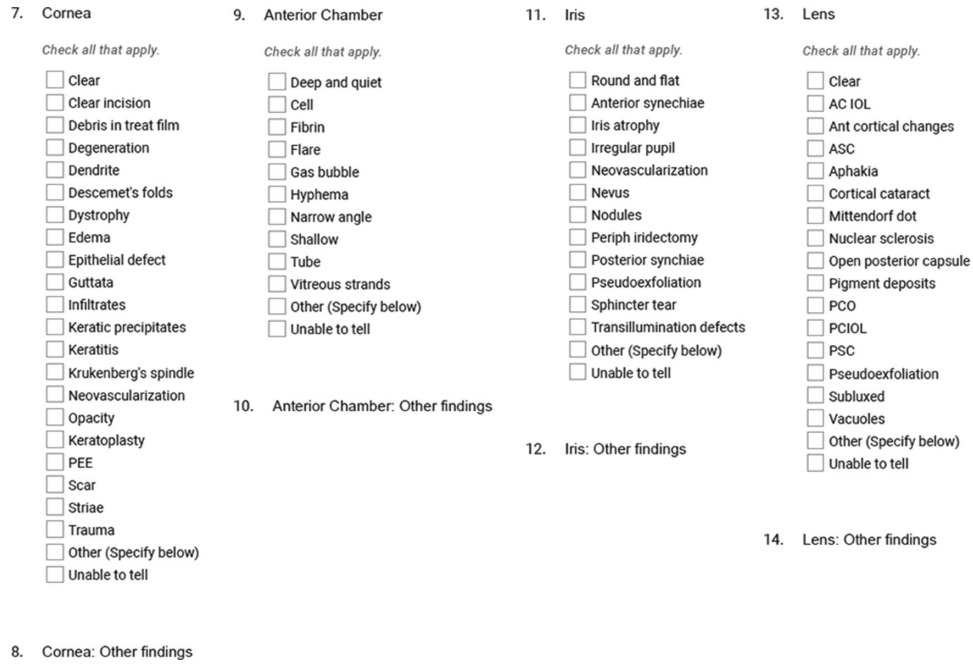

Figure 8. Example of evaluation form for eye structures: cornea, anterior chamber, iris and lens.

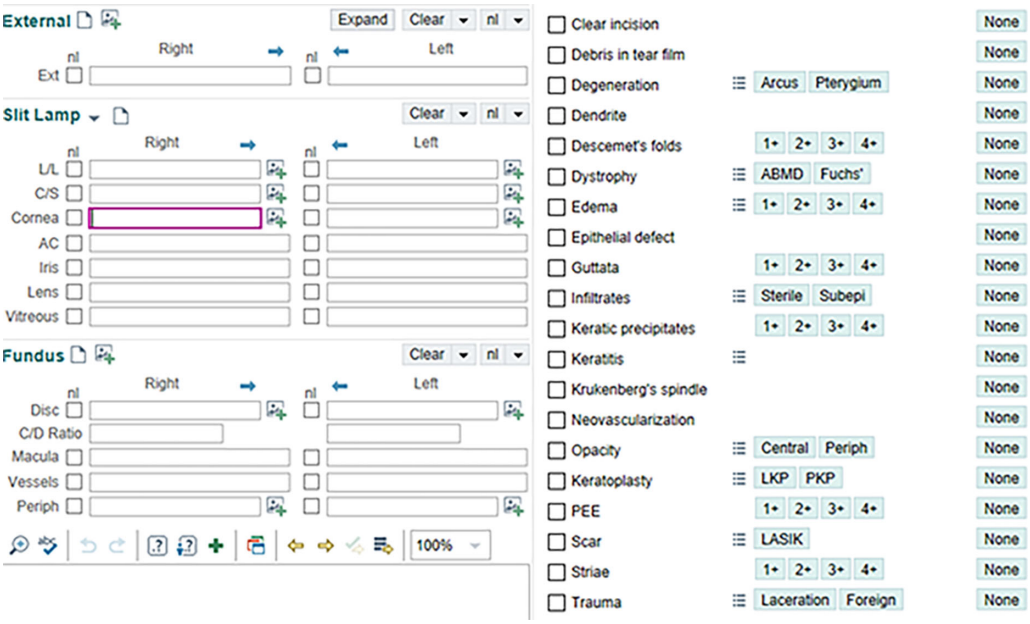

Figure 9. Example of evaluation form used in the electronic medical records for evaluating the cornea.

were determined. A Z-test for two sample proportions was performed to analyze the significance of the specificity and sensitivity percentages between modalities. The significance value was 0.05 and the 2 tailed *P* value was reported. The average image quality grade for each imaging system was calculated from the grading question.

Results

The overall sensitivity and specificity percentages were calculated. The wearable headset camera system's percentage sensitivity and specificity were 33.3% and 78.1%, respectively. However, the web camera evaluations had a 14.6% sensitivity and a 56.2% specificity. The Z-test for two proportions comparing the sensitivity percentages of the headset video evaluations and web camera evaluations resulted in a $P = 0.001$. The Z-test comparing the specificity evaluations between the two modalities resulted in a $P < 0.001$. These results are presented in Table 1.

The sensitivity and specificity of ocular features were also calculated. Table 2 summarizes the comparison between the imaging modalities and the clinical

Table 1. Overall Sensitivity and Specificity Percentages and Z-Test Results for Headset Camera System and Web Camera

N	P	Imaging Modality	TN	TP	FN	FP	UT	OC	Sensitivity (%)	Specificity (%)	Z-Test Two Proportions *P* Value Sensitivity	Z-Test Two Proportions *P* Value Specificity
137	108	Wearable headset	107	36	38	19	32	13	33.33	78.10	0.001*	$P < 0.001$*
		Web camera	77	16	27	19	93	13	14.81	56.20		

Note: This table presents the general sensitivity and specificity percentages calculated from the evaluations of the two imaging modalities and the clinical examination form, and the p-values that results from the z-test of two proportions analysis.

N, number of not diseased evaluations in the clinical chart; P, number of diseased evaluations in the clinical chart; TN, true negative, TP, true positive; FN, false negative; FP, false positive; UT, unable to tell; OC, other condition.

*Statistically significant.

Table 2. Wearable Headset Camera Systems and Web Camera Clinical Findings by Ocular Features

Ocular Structures	N	P	Imaging Modality	TN	TP	FN	FP	UT	OC	Sensitivity (%)	Specificity (%)
External	33	2	Wearable headset	26	0	1	5	3	0	0.00	78.79
			Web camera	23	1	1	9	1	0	50.00	69.70
Lids and lashes	17	18	Wearable headset	12	2	12	4	0	5	11.11	70.59
			Web camera	12	2	8	4	4	5	11.11	70.59
Conjunctiva and sclera	20	15	Wearable headset	13	10	1	6	0	5	66.67	65.00
			Web camera	12	8	3	6	2	4	53.33	60.00
Cornea	9	26	Wearable headset	8	12	11	1	1	2	46.15	88.89
			Web camera	6	4	12	0	9	4	15.38	66.67
Anterior chamber	27	8	Wearable headset	22	4	1	2	5	1	50.00	81.48
			Web camera	12	0	0	0	23	0	0.00	44.44
Iris	24	11	Wearable headset	22	1	7	1	4	0	9.09	91.67
			Web camera	12	1	3	0	19	0	9.09	50.00
Lens	7	28	Wearable headset	4	7	5	0	19	0	25.00	57.14
			Web camera	0	0	0	0	35	0	0.00	0.00

Note: This table presents the sensitivity and specificity percentages calculated from the video's evaluations and clinical examination form for each ocular structure.

N, number of not diseased evaluations in the clinical chart; P, number of diseased evaluations in the clinical chart; TN, true negative; TP, true positive; FN, false negative; FP, false positive; UT, unable to tell; OC, other condition.

findings by ocular structures. An overview of the results reveals that for each ocular structure the specificity percentages are higher than sensitivity percentages in both imaging modalities. On the other hand, Table 2 demonstrates that the videos' evaluations from the headset camera system had higher sensitivity and specificity percentages when assessing the conjunctiva, cornea, anterior chamber, iris, and lens. Their specificity percentages ranged from 57.1% to 91.7%, and sensitivity percentages ranged from 9% to 50%. Whereas for the web camera, the specificity percentage for the same features were less than 66.7%, and the sensitivity percentage was 15.4% for the cornea, and no pathology was identified in the other 3 ocular features. Only 2 of the 18 positive conditions observed in the clinical examination for the lids and lashes were identified with both imaging system. The evaluations of the conjunctiva and sclera had the highest sensitivity percentage for both imaging modalities (66.7% wearable headset camera and 53.3% web camera). Furthermore, the statistical significance of the sensitivity and specificity percentages of the modalities were calculated using a Z-test for two proportions. Results are presented in Table 3. The analysis of the P values obtained showed statistically significant differences in the sensitivity percentage for the cornea ($P = 0.016$), anterior chamber ($P = 0.021$), and lens ($P = 0.005$), and the specificity percentage for the anterior chamber ($P = 0.005$), iris ($P = 0.001$), and lens ($P = 0.018$).

In the form given to the doctors, the option to mark an UT box whenever they considered that video did not allow for the evaluation of an ocular feature was provided. As presented in Table 1, 93 out of the possible 245 evaluations (38%) were marked as UT using the web camera videos, and only 32 (13.1%) were marked UT with the wearable headset camera videos. A closer look in Table 2 shows 82.79% of the web camera and all UT evaluations of the new imaging system corresponded to the ocular structures of the anterior chamber, iris, and lens.

Table 4 presents the pathologies identified with the videos from the wearable headset and the web camera system. The new imaging system allowed the identification of more pathologies for the cornea, anterior chamber, and lens. The conditions identified with this system included PCIOLs, nuclear sclerosis, keratitis, keratoplasty, and a hypopyon among others.

Another assessment in this study included evaluating the video/image quality based on the grader's ability to identify emergent findings from the videos. The graders evaluated each of the videos using the scale from 1 to 5 is explained under the Methods sections. The average grade for the developed camera system and the web camera evaluations was 3, indicating that the doctors were only able to exclude emergent findings with the videos.

Table 3. Z-Test for Two Proportions to Compare Sensitivity and Specificity Percentages Between Imaging Modalities

Ocular Structures	Imaging Modality	Sensitivity (%)	Specificity (%)	Z-Test Two Proportions *P* Value Sensitivity	Z-Test Two Proportions *P* Value Specificity
External	Wearable headset	0.00	0.00	1.752	0.398
	Web camera	50.00	69.70		
Lids and lashes	Wearable headset	11.11	70.59	1.000	1.000
	Web camera	11.11	70.59		
Conjunctiva and sclera	Wearable headset	66.67	65.00	0.456	0.744
	Web camera	53.33	60.00		
Cornea	Wearable headset	46.15	88.89	0.016*	0.257
	Web camera	15.38	66.67		
Anterior chamber	Wearable headset	50.00	81.48	0.021*	0.005*
	Web camera	0.00	44.44		
Iris	Wearable headset	9.09	91.67	1.000	0.001*
	Web camera	9.09	50.00		
Lens	Wearable headset	25.00	57.14	0.005*	0.018*
	Web camera	0.00	0.00		

Note: This table the results from a Z-test of two proportions that compares the sensitivity and specificity percentages between the headset camera system and the web camera.

*Statistically significant.

Table 4. List of Pathologies Identified in the Video Evaluations From the Wearable Headset Imaging System and the Web Camera

	Pathologies Identified by	
Ocular Structures	Wearable Headset	Webcam
External		Edema
Lids and lashes	Tarsorrhaphy	Tarsorrhaphy
	Blepharitis	
	Ptosis	Ptosis
Conjunctiva and sclera	Injection	Injection
	Bleb	
Cornea	Opacity	Opacity
	Infiltrates	Infiltrates
	Keratoplasty	
	Keratitis	
	PEE	
	Corneal thinning	
Anterior chamber	Hypopyon	
	Formed	
Iris	Irregular pupil	Irregular pupil
Lens	PCIOL	
	Nuclear sclerosis	

Discussion

This study assessed the accuracy and reliability of performing eye evaluations based on the videos obtained from a wearable headset camera system and a computer web camera. These evaluations were compared with the standard clinical assessment performed by an ophthalmologist with a slit-lamp biomicroscope during the clinical visit.

Results showed that the evaluations for both imaging modalities had high specificity but low sensitivity. Overall, eye evaluations from the videos have low accuracy in screening for pathologies. On the other hand, the evaluations performed from the videos recorded with the wearable headset camera system had statistically significantly higher specificity and sensitivity than the evaluations obtained from webcam videos. Similarly, the specificity and sensitivity values were higher in the headset camera system than in the webcam for all ocular features. However, significant differences were only seen in the cornea, anterior chamber, iris, and lens evaluations. Moreover, the number of UT evaluations was highest in the webcam videos, and the greatest percentage was seen when evaluating the cornea, iris, anterior chamber, and lens. Therefore, the wearable headset camera system allowed better evaluation of these eye

structures than the current telemedicine eye evaluation standard, but not as significant as the clinical examinations.

In a similar study performed in Perth, Australia, at the Lion Eye Institute, researchers compared the detection of anterior segment disorders from still digital images between a portable slit-lamp camera and the standard slit lamp biomicroscope with the traditional clinical assessment.[7] This research studied 392 eyes, and 33 specific conditions were identified. The measured specificity percentages ranged from 98% to 99% for the portable imaging system. However, according to researchers, a low prevalence in many categories of anterior segment conditions limited the study, and the sensitivity and specificity percentages are not particularly useful when less than five subjects have a specific condition. This is a similar issue encountered in our study, where few of the identified conditions were not present in multiple patients. In addition, in the Lion Eye Institute research, three ophthalmologists evaluated all the patients; therefore, in our future studies, doctors should evaluate all patients to better compare inter subject agreement. In summary, they determined that standardized views of still images did not compare with the clinical examinations, because the cameras did not offer a full view of eyelids and conjunctiva and had a shallow depth of focus. The prototype presented in this study addresses some of these issues by analyzing videos instead of still images, allowing control of the camera focus, and adjusting camera position and lighting conditions. These features can be utilized to improve evaluation of different ocular structures.

Another study compared the photographs captured with an iTouch 5G smartphone camera (Apple, Cupertino, CA) and a portable diffuse light ophthalmic camera (Nidek, Fremont, CA), to the gold standard slit lamp and corneal specialist examination for diagnosing corneal pathologies.[8] Three ophthalmologists evaluated the images from the two cameras. The smartphone camera had a sensitivity range from 54% to 71% and a specificity range from 82% to 96%. The portable ophthalmic camera sensitivity ranged from 66% to 75%, and specificity from 91% to 98%. Similarly, this study discusses the presence of high specificity and low sensitivity percentages obtained when evaluating eye conditions from images. The standard for accuracy of telemedicine screening for diabetic retinopathy and other ophthalmic diseases requires a sensitivity percentage of at least 80%. A high sensitivity is required because it determines the accuracy of the imaging modality to capture ocular pathologies, especially in telemedicine that relies on images for remote evaluations. In the study presented in this paper, this sensitivity percentage limit was not achieved from the video evaluations.

The difference in video quality could be a factor that affected the results. For instance, the wearable headset camera system had a good resolution, however, the camera highest resolution could not be achieved because of a Raspberry Pi video memory restriction. In addition, even though LEDs aided with illumination, sometimes they created reflections and over-saturated images that affected video quality.

Moreover, the Arducam cameras focus could be adjusted, and because they were placed at eye level and near the eyes, a closer view could be obtained. However, the web camera video quality was limited by a fixed focus and a longer working distance. On the other hand, when taking videos with the web camera, the room illumination was another factor that limited video quality. Standardizing lighting conditions was challenging. The computer was left in the same position and usually patients were able to move forward and bring themselves closer to the camera. However, for some patients, the laptop had to be move toward them because they had difficulty seeing and moving around. Therefore, proper lighting conditions were not always achieved when recording with the web camera.

The correct positioning of the headset camera system was essential to obtain good videos. However, this was not always achieved. Factors that influence these differences included the physiognomy of the patients, how the headset fits on the patient's head, and the inter-pupillary distance. These are aspects that must be included in the development of the next camera prototype. During this study, the cameras were fixed to the center of each display on the headset glasses, and a ball-and-socket structure allowed for angle adjustment; as a result, sometimes the cameras were not centered correctly in the eye. For future prototypes, a motorized camera system can assist in the correct alignment and positioning of the cameras. In addition, the development of a slit-lamp illumination system will be better to improve the assessment of corneal pathologies and other anterior eye segment features. A new program will be developed to improve user interphase, a site where doctors can access real-life camera feedback and modify the camera position remotely. However, this initial prototype and study shows the application of AR/VR headsets in teleophthalmology for imaging the eye.

The comparison of the averaged video quality grade between to two imaging modalities showed that the videos allowed doctors to exclude only emergent findings. Even though the videos from the wearable system were expected to have a higher image quality grade, the averaged grade for both imaging systems

was the same. This could be the result of having different graders evaluating only a set of different videos. The image grade quality is a subjective assessment, therefore, in a future study, a quantitative method for measuring image quality could be included to compare the two systems.

Future studies need to compare the evaluation performed with the new wearable camera prototype with other portable camera systems such as smartphones with camera adaptors, because these are other common devices utilized in teleophthalmology. In addition, it will be good to compare evaluations from still images obtained with the wearable headset system with evaluations from still images obtained with a slit lamp biomicroscope. In addition, to improve the study design and the sensitivity of the video evaluations, more patients with a diverse set of ocular pathologies should be considered.

In summary, this study presents the development of a portable and autonomous prototype for anterior eye segment imaging, with a potential application in teleophthalmology. The analysis of the results shows that this new system is better for eye evaluations than the current standard for teleophthalmology that comprises of computer webcams. However, this system needs further improvement to provide a similar assessment to clinical evaluations.

Acknowledgments

Supported by a National Eye Institute Center Core Grant to the University of Miami (P30 EY014801), and Research to Prevent Blindness (RPB). The funding organization had no role in the design or conduct of this research.

Disclosure: **A. Diego**, None; **M. Abou Shousha**, United States Non-Provisional Patent (Application No. #20190094552). Patent is owned by University of Miami and licensed to Heru, Inc. MAS is an officer, equity holder and sits on the Board of Directors of Heru, Inc.

References

1. Parikh D, Armstrong G, Liou V, Husain D. Advances in Telemedicine in Ophthalmology. *Semin Ophthalmol*. 2020;35:210–215.
2. Saleem SM, Pasquale LR, Sidoti PA, Tsai JC. Virtual Ophthalmology: Telemedicine in a COVID-19 Era. *Am J Ophthalmol*. 2020;216:237–242.
3. Woodward MA, Bavinger JC, Amin S, et al. Telemedicine for ophthalmic consultation services: use of a portable device and layering information for graders. *J Telemed Telecare*. 2017;23(2):365–370.
4. Chen DZ, Tan CW. Smartphone Imaging in Ophthalmology: A Comparison with Traditional Methods on the Reproducibility and Usability for Anterior Segment Imaging. *Ann Acad Med Singapore*. 2016;45(1):6–11.
5. Hu WF, Lorch AC. Teleophthalmology For Anterior Segment Disease. *Int Ophthalmol Clin*. Fall 2019;59(4):55–67.
6. Mohammadpour M, Heidari Z, Mirghorbani M, Smartphones Hashemi H., tele-ophthalmology, and VISION 2020. *Int J Ophthalmol*. 2017;10(12):1909–1918.
7. Kumar S, Yogesan K, Constable IJ. Telemedical diagnosis of anterior segment eye diseases: validation of digital slit-lamp still images. *Eye (Lond)*. 2009;23(3):652–660.
8. Woodward MA, Musch DC, Hood CT, et al. Teleophthalmic Approach for Detection of Corneal Diseases: Accuracy and Reliability. *Cornea*. 2017;36(10):1159–1165.
9. Ludwig C, Murthy S, Pappuru R, Jais A, Myung D, Chang R. A novel smartphone ophthalmic imaging adapter: User feasibility studies in Hyderabad, India. *Indian J Ophthalmol*. 2016;64(3):191–200.